Multichannel feedforward active noise control system with optical laser microphone in reverberant environments

Maoto Mizutani*, Kenta Iwai†, Masato Nakayama*, Takanobu Nishiura* and Yoshiharu Soeta‡
* Ritsumeikan University, Osaka, Japan
E-mail: {is0580kk@ed, mnaka@fc, nishiura@is}.ritsumei.ac.jp
† Osaka Sangyo University, Osaka, Japan
E-mail: iwai@ise.osaka-sandai.ac.jp
‡ National Institute of Advanced Industrial Science and Technology (AIST), Ikeda, Japan
E-mail: y.soeta@aist.go.jp

***Abstract*—A feedforward active noise control (ANC) system is affected by a constraint related to processing and sound propagation delay, known as the causality constraint. To address this problem, an ANC system incorporating an optical laser microphone has been proposed. The optical laser microphone captures the vibration velocity of the target noise at the speed of light, thereby relaxing the causality constraint. However, the acquired signal contains few components related to the reverberation characteristics of the room. As a result, the noise reduction performance of the system degrades in reverberant environments. To overcome this issue, we propose a multichannel feedforward active noise control system to improve the noise reduction performance in reverberant environments. The proposed system uses both an optical laser microphone and an air-conducted microphone as reference microphones. The key feature of the system is the additional air-conducted microphone, which acquires the noise with the reverberant components. The system processes signals acquired by each microphone using each noise control filter, thereby both relaxing the causality constraint and accounting for the room's reflective characteristics. As a result of actual experiments, we confirmed that the proposed system improves the noise reduction performance.**

I. Introduction

Active noise control (ANC) systems offer an effective solution to reducing unwanted noise [1]–[3]. Figure 1 illustrates the basic principle of an ANC system. Based on the principle of sound wave superposition [1]–[3], ANC systems minimize the unwanted noise by generating a control signal with the same amplitude but opposite phase to the unwanted noise at a specific cancellation point.

A feedforward ANC system has been proposed as an effective technique for attenuating unwanted noise [1]–[3]. This approach consists of a reference microphone, an error microphone, and a secondary loudspeaker. However, its noise reduction performance is limited by a constraint related to processing and propagation delays, known as the causality constraint [4]. If this constraint is not satisfied, the noise reduction performance of the system deteriorates significantly.

To address this limitation, a feedforward ANC system incorporating an optical laser microphone has been proposed [5].

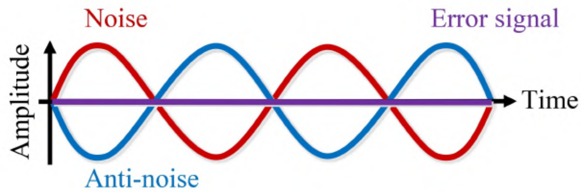

Fig. 1. Principle of the ANC system.

In this configuration, the optical laser microphone [6] replaces the air-conducted microphone that was previously used as the reference microphone. Because it measures the vibration velocity of the noise source with light-speed responsiveness, it can significantly relax the causality constraint. However, due to its physical properties, the optical laser microphone cannot capture reverberant components at all. As a result, the noise reduction performance of the system degrades in high-reverberant environments.

To overcome this issue, in this paper, we propose a multichannel feedforward ANC system that utilizes both an optical laser microphone and an air-conducted microphone. In the proposed system, reference signals from each microphone are processed independently through two dedicated noise control filters. This configuration not only mitigates the causality constraint but also compensates for the reverberation characteristics of the room. Finally, we evaluate the noise reduction performance of the proposed system through actual experiments. Moreover, in this paper, a laser Doppler vibrometer (LDV) and an electret condenser microphone (ECM) are used as the optical laser microphone and the air-conducted microphone, respectively.

II. Feedforward ANC System

Figure 2 shows the structure of a feedforward ANC system. In Fig. 2, the primary path refers to the path from the noise source to the error microphone; the reference path is the path from the noise source to the reference microphone; and the secondary path represents the path from the secondary

979-8-3315-7206-8/25/$31.00

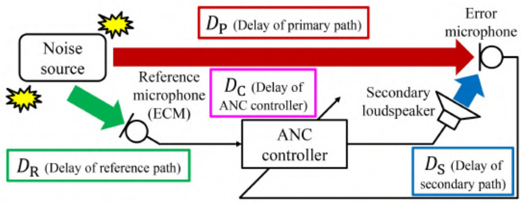

Fig. 2. Structure of the feedforward ANC system.

loudspeaker to the error microphone.

In the feedforward ANC system, the unwanted noise is initially acquired by the reference microphone. The captured signal, known as the reference signal, is used to adaptively update the noise control filter. The reference signal is obtained as the noise propagates through the reference path. Using the reference signal, a control signal is generated by the ANC controller after the filter update. This control signal is then sent to the secondary loudspeaker, which emits anti-noise that aims to cancel the unwanted noise reaching the error microphone via the primary path.

To update the noise control filter, adaptive algorithms such as the filtered-x least mean square (FxLMS) or the filtered-x normalized least mean square (FxNLMS) algorithm are typically used [7].

However, the feedforward ANC system is affected by a constraint related to processing and sound propagation delay, known as the causality constraint [4]. If this constraint is not satisfied, the noise reduction performance of the system deteriorates. In Fig. 2, the following delays occur:

D_{P}: propagation delay of the sound from the noise source to the error microphone (primary path)

D_{R}: propagation delay of the sound from the noise source to the reference microphone (reference path)

D_{C}: processing delay of the ANC controller, including filter adaptation and control signal generation

D_{S}: propagation delay of the anti-noise from the secondary loudspeaker to the error microphone (secondary path)

The causality constraint can be formulated as:

$$D_{\mathrm{P}} - D_{\mathrm{R}} \quad > \quad D_{\mathrm{C}} + D_{\mathrm{S}}, \tag{1}$$

where indicates that the control signal must reach the cancellation point before the original noise reaches the error microphone for effective noise cancellation. Therefore, the spatial distance between the reference and error microphones must be sufficiently long to allow enough time for signal processing and anti-noise propagation.

However, in actual applications, it is often challenging to meet this constraint due to limitations in microphone placement. To address this issue, we have proposed the feedforward ANC system employing an optical laser microphone as the reference microphone [5].

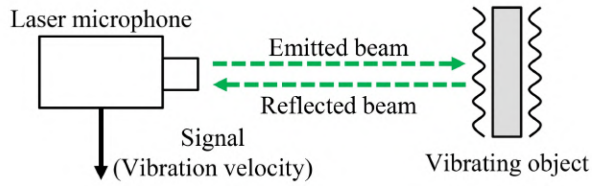

Fig. 3. Measurement principle of the optical laser microphone.

III. Conventional Feedforward ANC System with Optical Laser Microphone

A. Measurement Principle of Optical Laser Microphone

An optical laser microphone measures sound waves in terms of vibration velocity by directing a laser beam onto the surface of a vibrating object [6]. Figure 3 illustrates the measurement principle of the optical laser microphone. The emitted laser beam is reflected by the vibrating surface and received by an optical sensor within the microphone. Due to the Doppler effect, the frequency of the reflected beam shifts, while the frequency of the emitted beam remains constant. The vibration velocity is then calculated based on the frequency difference between the emitted and reflected laser beams.

B. Feedforward ANC System with Optical Laser Microphone

In a feedforward ANC system with an optical laser microphone [5], the optical laser microphone serves as the reference microphone. This type of microphone enables the acquisition of vibration velocity with light-speed responsiveness [6], thereby significantly relaxing the causality constraint.

Figures 4 and 5 show the structure and block diagram of the feedforward ANC system with the optical laser microphone. In Fig. 5, P denotes the primary path from the noise source to the error microphone, R_{LDV} represents the reference path from the noise source to the optical laser microphone, S indicates the secondary path from the secondary loudspeaker to the error microphone, W_{LDV} is the noise control filter, $\hat{S}$ is the secondary path model, and H_{D} denotes the first-order differentiator.

Next, the processing flow of the feedforward ANC system with the optical laser microphone is presented. In this paper, scalar quantities represent discrete-time signals at each time index n, whereas boldface vectors denote sequences of past and/or current samples arranged in vector form. First, the unwanted noise $v(n)$ is acquired using the reference microphone. The acquired reference signal, $x_{\mathrm{LDV}}(n)$, is then passed through a first-order differentiator based on the theoretical relationship between the volume velocity of a point source and sound pressure [5]. Since the reference microphone measures vibration velocity whereas the error microphone measures sound pressure, their frequency responses differ, which reduces coherence and degrades noise reduction performance. To compensate for this discrepancy, the first-order differentiator is applied to the reference signal, aligning it more closely with the characteristics of the error signal and thereby improving coherence and enhancing control performance [5]. The resulting differentiated signal, $x_{\mathrm{D,LDV}}(n)$, is processed by

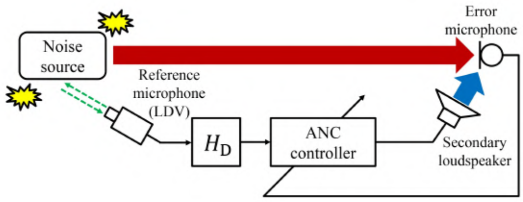

Fig. 4. Structure of the feedforward ANC system with the optical laser microphone.

the noise control filter $\boldsymbol{w}_{\mathrm{LDV}}(n)$ to produce a control signal $y(n)$. This control signal is sent to the secondary loudspeaker, which emits anti-noise $y_{\mathrm{S}}(n)$ to cancel out the unwanted noise $d(n)$ traveling through the primary path. The error signal $e(n)$ received by the error microphone is given by

$$e(n) = d(n) - y_{\mathrm{S}}(n), \tag{2}$$

where $y_{\mathrm{S}}(n)$ is the anti-noise given by

$$y_{\mathrm{S}}(n) = \boldsymbol{s}^{\mathrm{T}}(n)\boldsymbol{y}(n), \tag{3}$$

$$y(n) = \boldsymbol{w}_{\mathrm{LDV}}^{\mathrm{T}}(n)\boldsymbol{x}_{\mathrm{D,LDV}}(n), \tag{4}$$

$\boldsymbol{s}(n)$ is the impulse response of the secondary path, $(\cdot)^{\mathrm{T}}$ denotes the transpose operator, $\boldsymbol{y}(n)$ is the control signal vector, and $\boldsymbol{x}_{\mathrm{D,LDV}}(n)$ is the vector form of the differentiated reference signal.

The coefficient vector of the noise control filter, $\boldsymbol{w}_{\mathrm{LDV}}(n)$, is updated using the FxNLMS algorithm [7] as follows:

$$\boldsymbol{w}_{\mathrm{LDV}}(n+1) = \boldsymbol{w}_{\mathrm{LDV}}(n) + \frac{\alpha e(n)\boldsymbol{x}_{\mathrm{S,LDV}}(n)}{\|\boldsymbol{x}_{\mathrm{S,LDV}}(n)\|^2 + \beta}, \tag{5}$$

$$x_{\mathrm{S,LDV}}(n) = \hat{\boldsymbol{s}}^{\mathrm{T}}(n)\boldsymbol{x}_{\mathrm{LDV}}(n), \tag{6}$$

where $x_{\mathrm{S,LDV}}(n)$ and $\boldsymbol{x}_{\mathrm{S,LDV}}(n)$ are the filtered reference signal and its corresponding vector, respectively. The symbol $||\cdot||^2$ represents the squared l_2 norm, α is the step-size parameter $(0 < \alpha < 2)$, β is the regularization parameter, and $\hat{\boldsymbol{s}}(n)$ is the impulse response of the secondary path model.

When this feedforward ANC system is applied to real-world environments such as factories, the error signal $e(n)$ contains not only the direct sound component but also reflected sound components. However, since the reference signal $x_{\mathrm{LDV}}(n)$ obtained from the optical laser microphone is relatively insensitive to reverberation, it cannot effectively acquire these reflected components. As a result, the noise reduction performance of the ANC system degrades in reverberant environments.

IV. Proposed Multichannel ANC System

To address the aforementioned issue, we propose a multichannel feedforward ANC system that utilizes both an optical laser microphone and an air-conducted microphone. The proposed system comprises two reference microphones, one secondary loudspeaker, and one error microphone. The optical

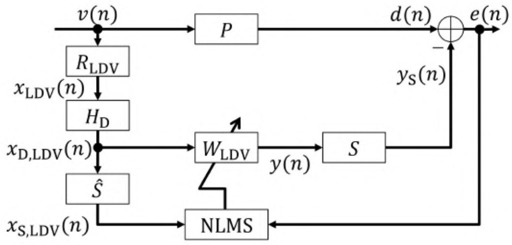

Fig. 5. Block diagram of the feedforward ANC system with the optical laser microphone.

laser microphone contributes to relaxing the causality constraint, while the air-conducted microphone captures reference signals that include room reverberation components.

Figures 6 and 7 illustrate the structure and block diagram of the proposed multichannel feedforward ANC system. In Fig. 7, R_{ECM} and R_{LDV} denote the reference paths from the noise source to the air-conducted and optical laser microphones, respectively. W_{ECM} and W_{LDV} represent the noise control filters applied to each reference signal. The signals $x_{\mathrm{ECM}}(n)$ and $x_{\mathrm{LDV}}(n)$ denote the reference signals from the air-conducted and optical laser microphones, respectively, while $x_{\mathrm{D,LDV}}(n)$ is the differentiated reference signal from the laser microphone. The corresponding filtered reference signals are denoted as $x_{\mathrm{S,ECM}}(n)$ and $x_{\mathrm{S,LDV}}(n)$.

The combined control signal $y(n)$ is expressed as:

$$y(n) = y_{\mathrm{ECM}}(n) + y_{\mathrm{LDV}}(n), \tag{7}$$

$$y_{\mathrm{ECM}}(n) = \boldsymbol{w}_{\mathrm{ECM}}^{\mathrm{T}}(n)\boldsymbol{x}_{\mathrm{ECM}}(n), \tag{8}$$

$$y_{\mathrm{LDV}}(n) = \boldsymbol{w}_{\mathrm{LDV}}^{\mathrm{T}}(n)\boldsymbol{x}_{\mathrm{D,LDV}}(n), \tag{9}$$

where $y_{\mathrm{ECM}}(n)$ and $y_{\mathrm{LDV}}(n)$ are the control signals corresponding to the reference signals acquired by the air-conducted and optical laser microphones, respectively.

The noise control filters are updated using the multiple-error filtered-x normalized least mean square (MEFxNLMS) algorithm [8]. The update equation is given by

$$\boldsymbol{w}_{l,j}(n+1) = \boldsymbol{w}_{l,j}(n) + \frac{\alpha \sum_{m=1}^{M} e_m(n)\boldsymbol{x}_{\mathrm{S},m,l,j}(n)}{\sum_{l=1}^{L}\sum_{j=1}^{J}||\boldsymbol{x}_{\mathrm{S},m,l,j}(n)||^2 + \beta}, \tag{10}$$

$$x_{\mathrm{S},m,l,j}(n) = \hat{\boldsymbol{s}}_{m,l}^{\mathrm{T}}\boldsymbol{x}_{\mathrm{S},j}(n), \tag{11}$$

where J, L, and M denote the maximum channel numbers of reference microphones, secondary loudspeakers, and error microphones, respectively. Here, $w_{l,j}(n)$ is the noise control filter, $\hat{\boldsymbol{s}}_{m,l}(n)$ is the impulse response of the secondary path model, and $x_{\mathrm{S},m,l,j}(n)$ and $\boldsymbol{x}_{\mathrm{S},m,l,j}(n)$ denote the filtered reference signal and its vector form, respectively. In this paper, we consider the case where $J = 2$, $L = 1$, and $M = 1$.

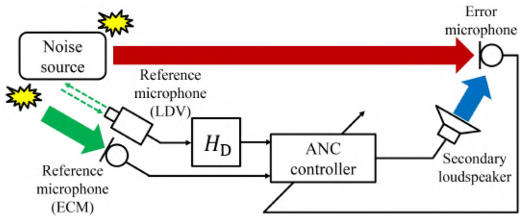

Fig. 6. Structure of the proposed ANC system.

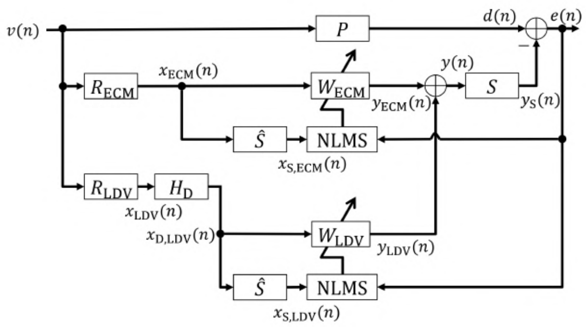

Fig. 7. Block diagram of the proposed ANC system.

V. Evaluation Experiment

We conducted real-world experiments to evaluate the noise reduction performance of the proposed ANC system. The noise reduction performance was compared across the following three systems:

1) A single-channel feedforward ANC system using the ECM denoted as the basic ANC,
2) A conventional single-channel feedforward ANC system using the LDV denoted as the conventional ANC,
3) The proposed multichannel feedforward ANC system using both microphones denoted as the proposed ANC.

A. Experimental Conditions

The experiments were conducted in two different environments:

- A soundproof room with a reverberation time of $T_{60} = 0.15$ s,
- An office room with a reverberation time of $T_{60} = 0.40$ s.

Figures 8 and 9 show the equipment layout and experimental setup in the soundproof environment. Similarly, Figures 10 and 11 depict the arrangement and environment for the experiments conducted in the office room. Table I presents the experimental conditions, and Figure 12 illustrates the system configuration. White noise was used as the noise source, and the ANC system was activated 10 seconds after the onset of the unwanted noise.

In this setup, the reference microphone with the LDV measures the vibration velocity of the noise source and is therefore unaffected by acoustic feedback from the secondary loudspeaker. In contrast, since the secondary loudspeaker and the reference microphone with the ECM were placed at a sufficient distance and the influence of acoustic feedback was considered negligible, no compensation or mitigation strategy was applied.

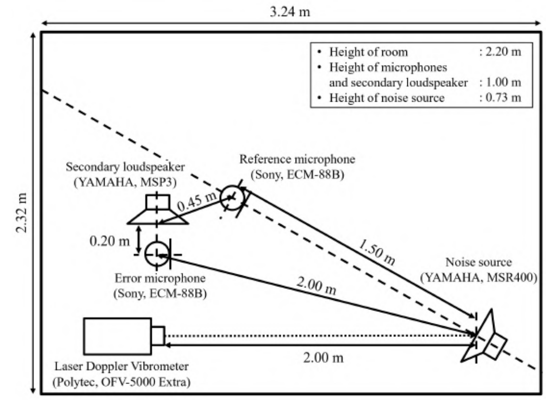

Fig. 8. Experimental arrangement in the soundproof environment.

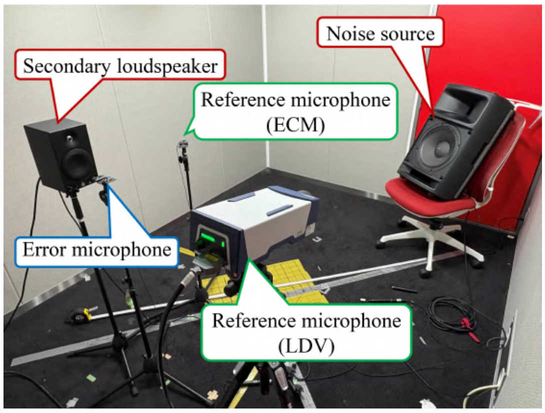

Fig. 9. Experimental environment in the soundproof environment.

B. Experimental Results

Figures 13 to 16 show the time-domain waveforms and spectrograms of the error signals for each ANC system in the respective environments. In addition, Table II summarizes the amount of noise reduction achieved in the real-world experiments. The noise reduction amount is defined as the difference in the average sound pressure level before and after the activation of the ANC system.

TABLE I
Experimental Conditions

Unwanted noise	White noise
Sampling frequency	8000 Hz
Frequency range	$60 - 2000$ Hz
Tap length of $\hat{S}$, W	300
Step size parameter	0.005
Update algorithm of adaptive filter (single-channel)	FxNLMS
Update algorithm of adaptive filter (multichannel)	MEFxNLMS
Regularization parameter	1.0×10^{-6}

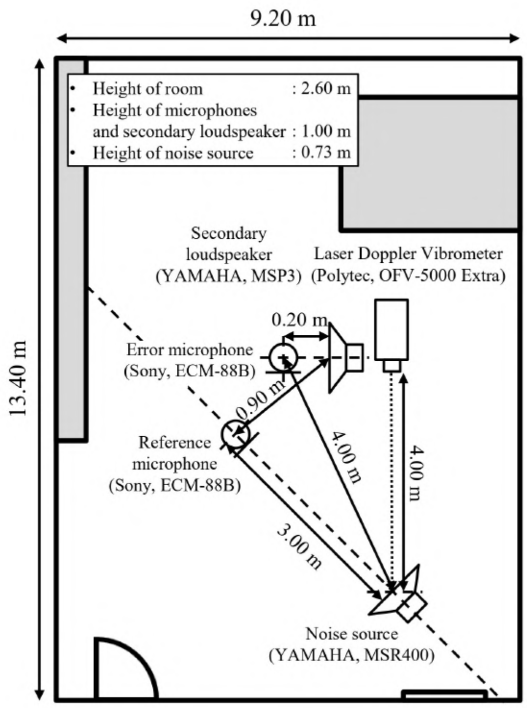

Fig. 10. Experimental arrangement in the office environment.

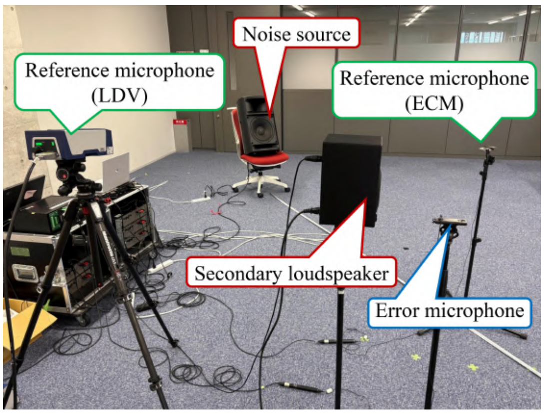

Fig. 11. Experimental environment in the office environment.

From Figures 13 and 14, it can be observed that the proposed system achieves the most significant reduction in unwanted noise. Furthermore, as shown in Table II, the proposed system achieves approximately 5.0 dB greater noise reduction than the conventional system in the soundproof environment and approximately 1.5 dB greater in the office environment.

On the other hand, Table II also indicates that the basic ANC system exhibits the lowest noise reduction performance in the office environment. This may be attributed to the fact that the system does not satisfy the causality constraint under these conditions.

Figures 15 and 16 further reveal that the proposed system achieves the highest noise reduction in the frequency range of 0–1000 Hz across both environments. This improvement may be due to the ECM capturing spatial reflection characteristics that are not present in the LDV signal, thus compensating for the limitations of the LDV in reverberant conditions.

Consequently, these results demonstrate that the proposed multichannel ANC system outperforms conventional ANC systems in real-world scenarios and maintains robust noise reduction performance across different acoustic environments.

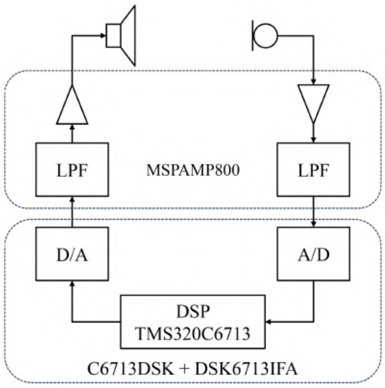

Fig. 12. Implementation of identification system.

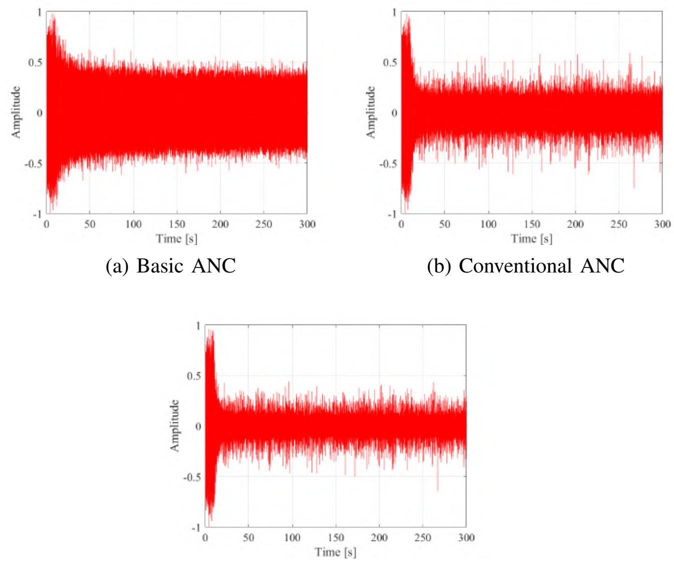

(a) Basic ANC (b) Conventional ANC

(c) Proposed ANC

Fig. 13. Time waveforms of error signals in the soundproof environment.

TABLE II
AMOUNT OF NOISE REDUCTION

ANC system	**Amount of noise reduction [dB]**	
	Soundproof environment	**Office environment**
Basic ANC	6.3	3.3
Conventional ANC	10.9	5.0
Proposed ANC	15.3	6.4

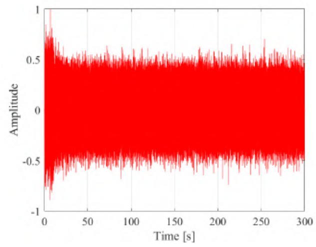

(a) Basic ANC

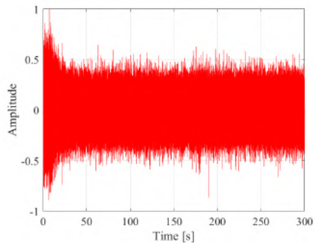

(b) Conventional ANC

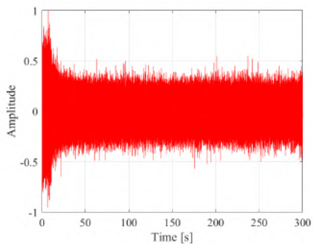

(c) Proposed ANC

Fig. 14. Time waveforms of error signals in the office environment.

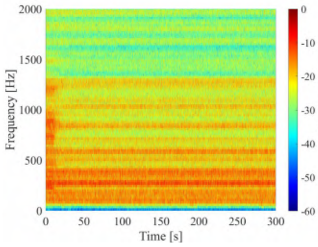

(a) Basic ANC

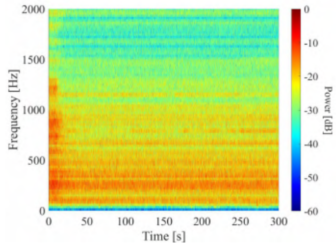

(b) Conventional ANC

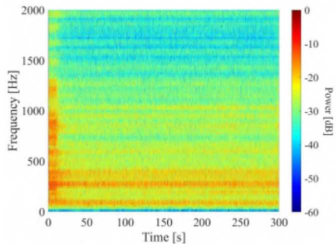

(c) Proposed ANC

Fig. 16. Spectrograms of error signals in the office environment.

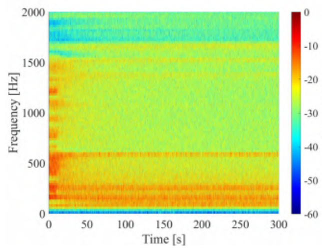

(a) Basic ANC

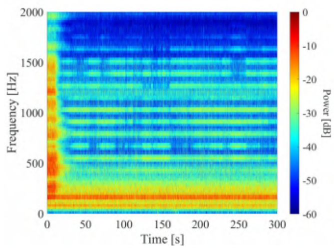

(b) Conventional ANC

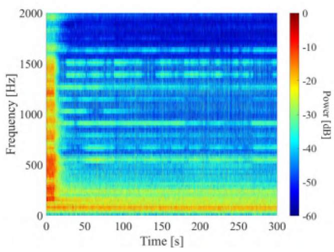

(c) Proposed ANC

Fig. 15. Spectrograms of error signals in the soundproof environment.

VI. Conclusion

In this paper, we proposed a multichannel feedforward active noise control (ANC) system that incorporates both an optical laser microphone and an air-conducted microphone, with the aim of improving noise reduction performance in reverberant environments. Real-world experiments using a digital signal processor demonstrated that the proposed system outperforms conventional ANC systems in terms of noise reduction. Furthermore, the results confirmed that the proposed system maintains its effectiveness across different acoustic environments.

As future work, we plan to develop an enhanced ANC system that integrates the current air-conducted reference microphone with a virtual sensing technique [9], which eliminates the need for physically installed microphones.

Acknowledgment

This work was partly supported by Ritsumeikan University R-GIRO, ARC and RARA, and JSPS KAKENHI Grant Numbers JP21K17773, JP23K28115 and JP25H01158.

References

[1] S. M. Kuo and D. R. Morgan, "Active Noise Control: A Turtorial Review," in proceedings of the IEEE, vol. 87, no. 6, pp. 943–973, 1999.
[2] Y. Kajikawa, W. S. Gan, and S. M. Kuo, "Recent advances on active noise control: open issues and innovative applications," APSIPA Transactions on Signal and Information Processing, vol. 1, pp. 1–21, 2012.
[3] B. Lam, W. S. Gan, D.-Y. Shi, M. Nishimura, and S. Elliott, "Ten questions concerning active noise control in the built environment," Building and Environment, vol. 200, pp. 1–18, 2021.
[4] X. Kong and S. M. Kuo, "Study of causality constraint on feedforward active noise control systems," IEEE Transactions on Circuits and Systems, vol. 46, no. 2, pp. 183–186, 1999.
[5] K. Iwai and T. Nishiura, "Feedforward active noise control system using optical laser microphone to overcome causality constraint," APSIPA Transactions on Signal and Information Processing, vol. 12, no. 1, pp. 1–23, 2023.
[6] R. Peng, C. Zheng, and X. Li, "Bandwidth extension for speech acquired by laser doppler vibrometer with an auxiliary microphone," in proceedings of 2015 10th International Conference on Information, Communications and Signal Processing, pp. 1–4, 2015.
[7] E. Bjarnason, "Analysis of the filtered-x LMS algorithm," IEEE Transactions on Speech and Audio Processing, vol. 3, no. 6, pp. 504–514, 1995.
[8] X. Liu, Q. Zou, X. Wang, and G. Lin, "Acoustic feedback effect reduction based on path compensation in multichannel FXLMS sound inhibition systems," in proceedings of 2014 5th International Conference on Digital Home, pp. 390–394, 2014.
[9] C. Shi, R. Xie, N. Jiang, H. Li, and Y. Kajikawa, "Selective virtual sensing technique for multi-channel feed-forward active noise control systems," in proceedings of 2019 IEEE International Conference on Acoustics, Speech and Signal Processing, pp. 8489–8493, 2019.